Critical currents in granular superconductors

J. W. Ekin*
Cryogenics Division, Institute for Basic Standards, National Bureau of Standards, Boulder, Colorado 80302
(Received 10 April 1975)

A relatively simple principle is experimentally demonstrated for producing extremely low critical-current density materials for application in quantum flux-flow devices. Essentially the technique consists of making the scale of structural disorder in the material small compared with the vortex core size. The smaller this ratio, the smaller the effects of bulk pinning, and the smaller the resulting critical-current density. Data for this study were obtained using superconducting granular aluminum films evaporated in a cylindrical geometry designed to eliminate edge-pinning effects. The data show J_c to exhibit a sharp minimum as a function of grain size, with the lowest values of J_c occurring in those films having the smallest ratio $\langle D\rangle/(\xi_0 l)^{1/2}$. Here $\langle D\rangle$ is the average grain size, ξ_0 is the BCS coherence length, and l is the electronic mean free path. The normal-state resistivity ρ_n can be used as an index of $\langle D\rangle/(\xi_0 l)^{1/2}$ for the granular aluminum system, with the lowest critical-current densities occurring in films prepared to have a ρ_n of about 10 $\mu\Omega$cm. In addition to discussing the dependence of the critical current on microstructure, data on the temperature dependence and electric field dependence of J_c are presented.

I. INTRODUCTION

Inhomogeneities in type-II superconductors such as dislocations and crystallites are an important source of vortex pinning. These defects alter the superconductor properties and serve as pinning sites for the vortex structure. A principal result of recent critical-current studies is that the strength of this pinning is, in most cases, directly proportional to the area of defect interface per unit volume.[1] That is, the more finely divided the structure, the stronger the pinning, and the higher the critical-current density.

This result holds, however, only up to the point where the defect size is made so small that it becomes comparable to the vortex-core diameter. In this experimental study it will be shown that further reduction of the defect size will lead to just the opposite relation: the smaller the scale of structural disorder, the *lower* the critical-current density. In particular, our data show that under these conditions the critical-current density J_c scales with the ratio $\langle D\rangle/\xi$, where $\langle D\rangle$ is the average size of defects occurring in the superconductor and ξ is the vortex-core dimension.[2] Minimization of this ratio can lead to extremely low critical-current densities and provides a relatively simple method to obtain materials with very low J_c for quantum flux-flow device applications. The method will be applied specifically to the granular aluminum film system[3] where it will be shown that there exists an optimum average grain size for which the critical-current density attains its lowest value.

II. SCALING OF J_c WITH $\langle D\rangle/\xi$

Consider the situation where the average defect size $\langle D\rangle$ in a superconductor is small compared with the vortex-core dimension ξ. In such case, each vortex core will span many defects and the net pinning potential acting on each vortex will be reduced to an average over the ensemble of inhomogeneities. The extent to which this averaging occurs is dependent on the number of defects spanned by the vortex core. That is, the smaller the *relative* defect size, the smaller the pinning. Thus it might be expected that the overall magnitude of J_c would scale approximately with the ratio of defect size to vortex-core size in the material, $\langle D\rangle/\xi$. This qualitative scaling feature can be more quantitatively justified by relating the critical current to correlation functions of the structural inhomogeneities in the superconductor. The precise dependence on $\langle D\rangle$ and ξ will vary depending on the particular theoretical approximations used, but a principal result of such an analysis is that the overall scaling of J_c is dominated by the relative size of these two quantities.

We now evaluate the ratio $\langle D\rangle/\xi$ for subsequent comparison with the critical-current data obtained on the granular aluminum film system. For this material, $\langle D\rangle$ is identified with the average grain size occurring in the film and will be a function of the conditions under which the film is evaporated. The lower the evaporation rate and the higher the partial pressure of oxygen during evaporation of these films (see Sec. IV), the smaller the resulting average grain size. The distribution of grain sizes in the granular aluminum system has been measured by Deutscher *et al.* using high-resolution dark-field electron microscopy.[4] The results show the average grain size to be a function of the film's normal-state resistivity ρ_n, essentially independent of the particular choice of rate and pressure used in preparing the film. This is fortunate for we may use a film's measured resistivity as an independent parameter to

determine $\langle D\rangle$ within the accuracy needed for the scaling comparisons made here.[5] The results for $\langle D\rangle$ are plotted as a function of ρ_n in Fig. 1.[4]

The size of the vortex core, on the other hand, is determined by the temperature-dependent coherence length ξ. Since the data for this study were obtained over a temperature range which did not extend too far below the critical temperature ($T/T_c \gtrsim 0.7$), and since the electronic mean free path l in these films is small by comparison with the BCS coherence length ξ_0, we approximate ξ by its dirty-limit evaluation in the Ginzburg-Landau theory, for which case

$$\xi(T) = 0.85\,(\xi_0 l)^{1/2}(1 - T/T_c)^{-1/2}\ . \tag{1}$$

Thus, for constant reduced temperature $1 - T/T_c$, $\xi(T)$ will be proportional to the factor $(\xi_0 l)^{1/2}$. To evaluate this term, l was obtained from the normal state resistivity using the relation[6]

$$\rho_n l = 0.4\times 10^{-11}\ \Omega\,\mathrm{cm}^2\ . \tag{2}$$

The critical temperature T_c for granular aluminum is enhanced over that for pure aluminum (see Fig. 1) and so ξ_0 was determined by scaling the pure aluminum BCS coherence length of 16 000 Å by the measured value of T_c for each film

$$\xi_0 = (16\,000\ \text{Å})\ (T_{c\,\mathrm{pure}}/T_c)\ . \tag{3}$$

The calculated results for $(\xi_0 l)^{1/2}$ are plotted in Fig. 1 as a long-dashed line.

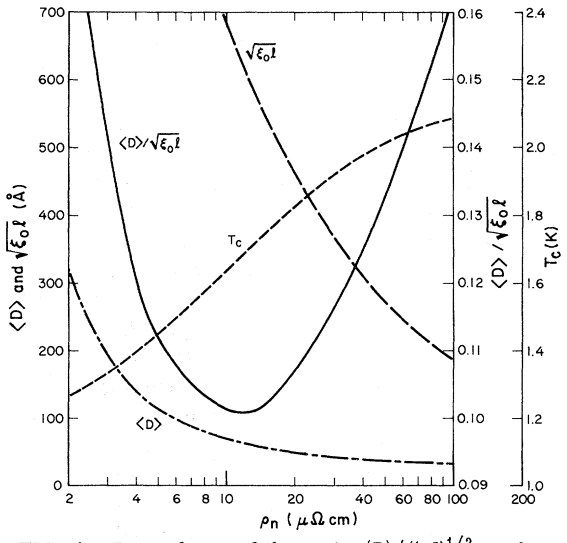

FIG. 1. Dependence of the ratio $\langle D\rangle/(\xi_0 l)^{1/2}$ on the normal-state resistivity for the granular aluminum system, showing the minimum at about 10 $\mu\Omega$ cm. Here $\langle D\rangle$ is the average grain size occurring in the film, ξ_0 is the BCS coherence length, l is the electronic mean free path, ρ_n is the normal-state resistivity at 4 °K, and T_c is the superconducting critical temperature.

Note from this figure that as the oxygen doping level is increased (i.e., ρ_n increased) not only does $\langle D\rangle$ decrease, but $(\xi_0 l)^{1/2}$ decreases as well, because the electronic mean free path is shortened. By taking the ratio of $\langle D\rangle$ to $(\xi_0 l)^{1/2}$, we obtain that part of $\langle D\rangle/\xi$ which is dependent on the material properties of the film. This is shown as a solid line in Fig. 1. Note that this ratio passes through a minimum at about 10 $\mu\Omega$ cm. Thus if the qualitative scaling argument outlined above is correct, we would expect the critical current density in the granular aluminum system to *pass through a minimum* as a function of oxygen doping level, with the lowest critical-current densities occurring in those films prepared to have $\rho_n \simeq 10$ $\mu\Omega$ cm.

III. EDGE-PINNING EFFECTS

Early in this study it was found that bulk pinning could be reduced to such an extent that edge pinning effects played a dominant role in determining the measured critical-current density. The situation is schematically illustrated in Fig. 2(a) which shows the usual planar sample geometry. A superconducting film placed perpendicular to an external magnetic field with a current applied along its length will experience a Lorentz force acting on the induced vortex structure.[7] This causes the flux lattice to try to move as a whole across the film with vortices being created at one edge and annihilated at the other. When bulk pinning is made extremely small, the interaction of the vortex lines with the Gibbs-free-energy barrier at each edge can dominate the total pinning potential acting on the vortex lattice. In fact, our earlier experiments showed the measured critical currents to vary by several hundred percent depending on the particular method used to define the sample edges, severely complicating any interpretation of the results.

This problem has been circumvented in the present study by simply eliminating the sample edges. Rather than planar samples, the films were evaporated on cylindrical substrates and placed in a radial magnetic field as illustrated in Fig. 2(b). The transport current was applied along the cylinder axis, resulting in continuous flux motion around the cylinder's circumference. The important point is that the flux lines never crossed any edges, eliminating this source of pinning.

The radial field for this experimental arrangement was produced by a permanent magnet constructed with concentric poles, as illustrated in Fig. 2(b).[8] A rod and concentric outer cylinder made of high permeability iron then served to transmit the magnetic flux out along the cylinder axis, generating a nearly uniform radial magnetic field in the annular gap formed between the rod and

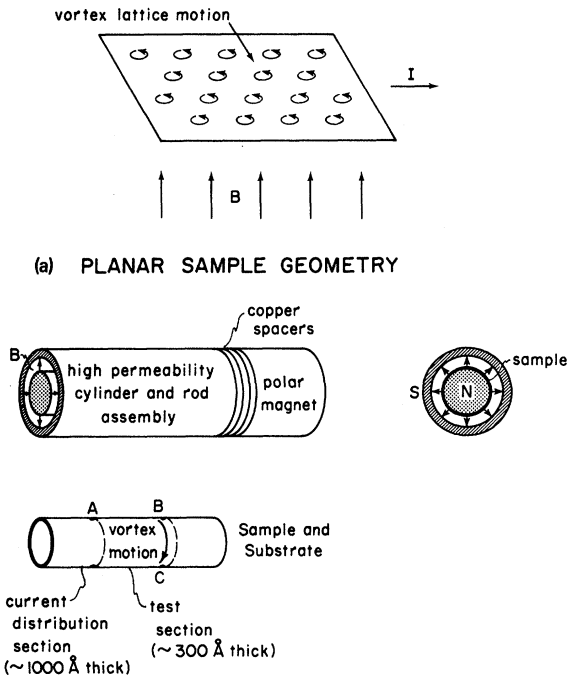

FIG. 2. (a) Schematic representation of vortex motion for the usual planar-sample geometry. (b) Continuously circulating vortex currents in the edge-free cyclindrical geometry. The sample was deposited on a cylindrical substrate and inserted in the annular gap formed by the high-permeability cylinder and rod. A radial field in the gap was generated by a permanent polar magnet; field magnitude was adjusted by inserting copper spacers between the magnet and cylinder arrangement. Homogeneity of the radial field in the region of the sample's test section was better than 95%.

cylinder. The field magnitude in the gap was set to 11.3 Oe for the measurements reported here by inserting copper spacer plates between the concentric-cylinder arrangement and the magnet. Field homogeneity in the region of the sample's test section was measured with a Hall probe to be better than 95%.

IV. SAMPLE PREPARATION

The granular aluminum system is particularly well suited for demonstrating critical-current scaling effects in the regime of small defect size since the BCS coherence length is relatively large, and it is not too difficult to obtain a granular structure whose average grain size is small compared with the vortex-core size. Furthermore, with this system, it is possible to obtain extremely thin, uniform, and stable films. We have observed the ~300-Å-thick samples used in this study to exhibit no deterioration from thermal shock or prolonged storage in air at room temperature.

The films were prepared by evaporating high-purity (59 grade) aluminum in an evaporator system equipped with a variable leak which was used to maintain a partial oxygen pressure of about 10^{-5} Torr. Film thickness and deposition rate (typically 10 Å/sec) were measured using a 6-MHz quartz crystal thickness monitor which was calibrated specifically for granular aluminum using a sodium-line interferometer. In order to obtain homogeneous films, care was taken to maintain a constant oxygen pressure and deposition rate during evaporation since the film properties are highly dependent on these parameters. Only relatively small variations in these quantities (factor of ~2) were required to produce films with normal-state resistivities spanning the range from about 10^{-6} to 10^{-4} Ω cm. The uncertainty in the thickness of ±5% constitutes perhaps the greatest error in the present experiment.

The substrates were cylindrical Pyrex glass tubes about 3 cm long and 1 cm in diameter, which were fire polished prior to deposition of aluminum on their outer surface. Fire polishing of the substrate surface was found to be essential to eliminate vortex pinning arising from residual contaminants and microscopic surface irregularities.

During evaporation the glass cylinder was rotated at several hundred rpm with a substrate-to-source distance of about 14 cm. The evaporation was started with the entire substrate exposed to the aluminum source. After a 300-Å-thick film had been deposited, the central section was masked by a shutter and the evaporation continued without interruption to build up thick sections at either end. These end sections were deposited under conditions such that they had a slightly enhanced T_c, their purpose being to distribute the current entering the center test section around the circumference.

The measurements were performed using a five-lead configuration with two current leads attached around the perimeter at each end of the specimen, and three voltage leads attached at points *A*, *B*, and *C* on either side of the thinner test section [see Fig. 2(b)]. Pure indium was used to spot solder the copper-voltage leads to the films. The extra voltage lead at point *C* was used to experimentally check that the current pattern was axial and that there was indeed an equipotential around the circumferences bordering the central section. For each of the samples in this study the voltage between points *A* and *B* was measured to be equal to that between points *A* and *C*.

V. ELECTRIC FIELD DEPENDENCE OF THE CRITICAL CURRENT

The voltage-current (*V*-*I*) characteristics obtained on the edge-free samples were found to have an ex-

tensive linear flux-flow region covering several decades of current and voltage. (Although not treated here, this is to be contrasted with the V-I characteristics which we measured for the planar geometry where the flux-flow region had a significant positive curvature over the same voltage range.) The extremely linear flux-flow region of the cylindrical samples made possible precise extrapolation of this straight-line section to zero voltage, uniquely determining the critical current. Note from this definition that we are concerned in this study with the dynamic critical current appropriate to relatively high flux-flow rates.

It should be mentioned, however, that this extrapolated value for the critical current may be quite distinct from the current at which voltage first appears. This is illustrated in Fig. 3 where the behavior of the V-I characteristics at relatively low electric field values is shown. The character of the low-voltage V-I relationship is a strong function of the reduced temperature and, as seen in Fig. 3, the current at the point of voltage onset can differ significantly from the dynamic critical current as defined above.

The shape of the V-I characteristic relatively near T_c is particularly interesting. If we use the

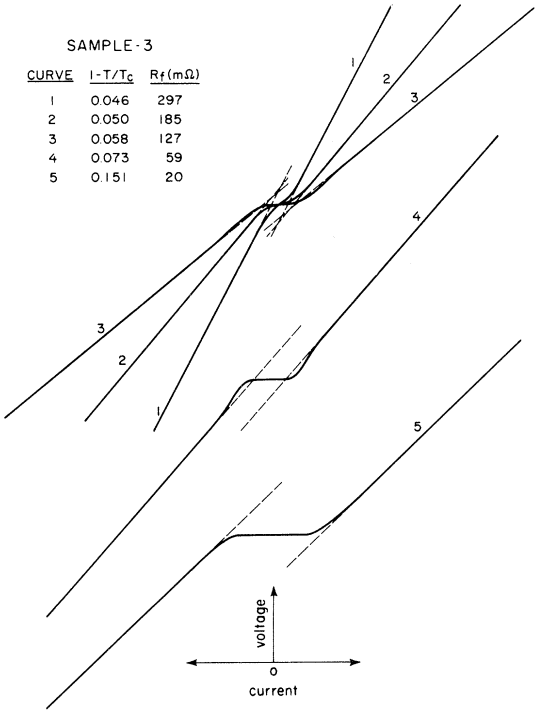

FIG. 3. Voltage-current characteristics of an edge-free film showing the shape of the characteristic near zero voltage at several reduced temperatures $1-T/T_c$. The straight-line sections of the characteristics extend well beyond the portions plotted. R_f is the flux-flow resistivity of these straight-line sections.

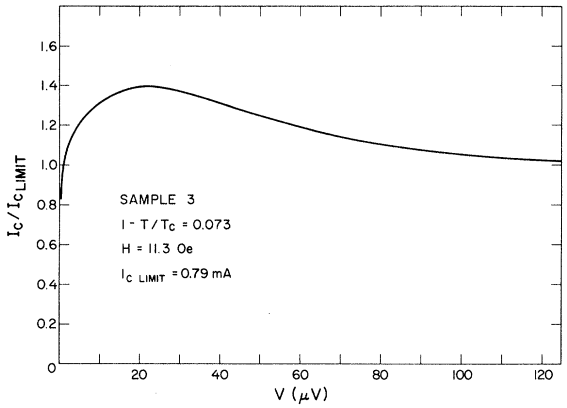

FIG. 4. Electric field dependence of the critical current relatively near T_c.

standard expression for the critical current

$$I = V/R_f + I_c \,, \tag{4}$$

where R_f is the flux-flow resistance, then we see that at low electric fields, I_c actually rises above its limiting dynamic value. This is illustrated

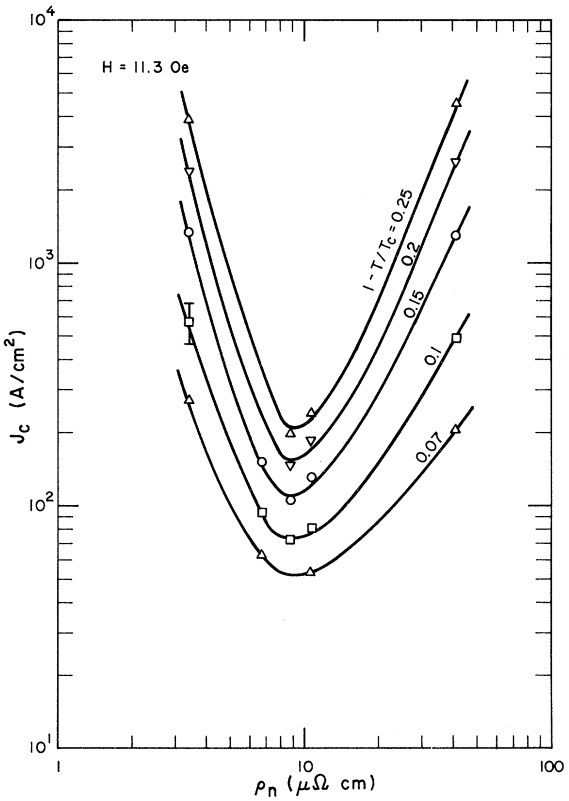

FIG. 5. Microstructure dependence of the critical current of granular aluminum. This figure is to be compared with Fig. 1 where the relative average grain size, $\langle D\rangle/\sqrt{\xi_0 l}$, is given as a function of the films's normal-state resistivity ρ_n.

TABLE I. Parameters characterizing the five samples studied in this work.

Sample	1	2	3	4	5
Film thickness (Å)	$d=290$	320	350	300	350
Normal resistivity at 4 °K ($\mu\Omega$ cm)	$\rho_n=41$	10.8	8.8	6.8	3.4
Electronic mean free path[a] (Å)	$l=9.8$	37	45	59	118
Critical temperature (K)	$T_c=1.95$	1.64	1.58	1.52	1.37
BCS coherence length[b]	$\xi_0=9800$	11 600	12 000	12 500	13 900
Upper critical field derivative[c] (Oe/K)	$\left(\frac{-dH_{c2}}{dT}\right)=2400$	650	540	410	200
Mean grain size[d] (Å)	$\langle D\rangle=38$	67	76	90	170

[a]Determined from ρ_n using Eq. (2).
[b]Determined from Eq. (3).
[c]Determined from Eq. (5).
[d]From G. Deutscher *et al.*, J. Low Temp. Phys. 10, 231 (1973).

more clearly in Fig. 4, where I_c for curve 4 in Fig. 3 has been plotted as a function of voltage. This enhancement of I_c at low electric fields is a feature that may be found in two recent critical current theories by Schmidt and Hauger[9] and by Larkin and Ovchinnikov,[10] which take into account deformations of the vortex lattice accompanying flux flow.

VI. EXPERIMENTAL PROCEDURE AND RESULTS

Parameters for the five samples studied are listed in Table I. Except for the critical temperature, most of these have already been discussed. The critical temperature was determined using the following procedure. Since the magnitude of the radial magnetic field was fixed at 11.3 Oe (see Sec. III) and not easily varied, each sample's resistivity was first measured as a function of temperature at this particular field.[11] The results served to determine the temperature at which $H_{c2}=11.3$ Oe. This temperature was extremely close to T_c and could easily be corrected with an iterative procedure to calculate T_c using the relation[12]

$$H_{c2}=\frac{\Phi_0}{2\pi(0.72)\xi_0 l}\,(1-T/T_c)\,, \qquad (5)$$

where Φ_0 is the quantum of flux. The magnitude of the correction was quite small and errors introduced by this procedure were less than 5 mK.

Measured values for the critical current density J_c are plotted in Fig. 5 as a function of each sample's normal-state resistivity ρ_n. Each curve corresponds to a different value of the reduced temperature $(1-T/T_c)$, and all were obtained at a constant magnetic field of 11.3 Oe.

The important point to note in this figure is that the critical current does indeed pass through a minimum as the normal state resistivity is increased, corroborating the predicted scaling of

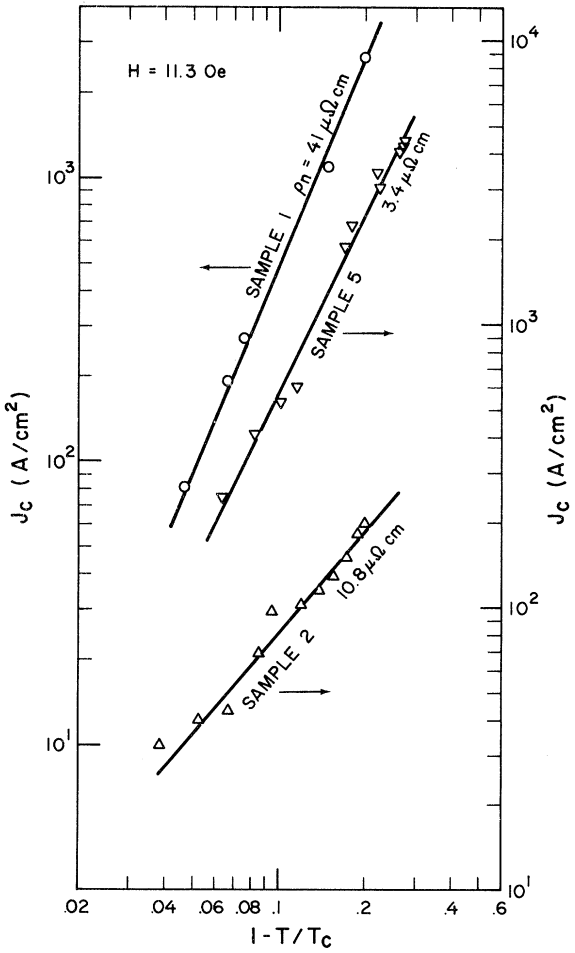

FIG. 6. Temperature dependence of the critical current. The data for sample 2 are typical of the temperature dependence for all the samples near the minimum in Fig. 5. Samples 1 and 5 on either side of the minimum were nearly identical and have been separated in the figure by using shifted scales.

J_c with the ratio $\langle D\rangle/(\xi_0 l)^{1/2}$ (see Sec. II). Moreover, the minimum value of J_c is observed to occur in the predicted range near 10 $\mu\Omega$ cm. The exact position of the minimum will depend on the detailed functional dependence of J_c on $\langle D\rangle$ and ξ individually, but the main point for the purposes of this paper is that the relative size of these two dimensions sets the range where this minimum will occur. Note also the sharpness of this minimum; on either side of the optimum oxygen-doping level, the critical-current density increases by more than an order of magnitude as ρ_n is varied by only a factor of ~3.

In Fig. 6 critical-current data are plotted for three of the samples in order to show the temperature dependence of J_c at the minimum (sample 2), compared to the dependence on either side of the minimum (samples 1 and 5). [The temperature dependence of the data for the other two samples (3 and 4) near the minimum were essentially identical to that shown for sample 2, but with a slight tendency to show the "peak effect"[13] very close to T_c, i.e., for values of $(1 - T/T_c)$ less than about 0.05.] Note that over the range of temperatures studied, J_c is a relatively pure power-law function of the reduced temperature, $(1 - T/T_c)^n$, with n varying from about 1 near the minimum to more than 2 on either side of the minimum.

VII. CONCLUSION

Data obtained on the granular aluminum system show that vortex pinning in these materials is a strong function of the relative size of two quantities: the average grain size $\langle D\rangle$ and the vortex-core dimension ξ. Extremely low bulk pinning can be obtained relatively easily by preparing materials in which the ratio of these two quantities $\langle D\rangle/\xi$ at constant reduced temperature is near minimum (provided $\langle D\rangle$ is less than ξ). This provides a relatively simple method of obtaining extremely low J_c materials for quantum device applications. In the granular aluminum system the optimum oxygen-doping level occurs for a 4 °K normal state resistivity of about 10 $\mu\Omega$ cm.

Bulk pinning in such films is reduced to such an extent that, even in relatively wide films spanning many vortices, edge-pinning effects play a dominant role in determining the critical current density. Data obtained on films that are free of edges, however, show a remarkably linear and extensive flux-flow regime. Such data also allow a clear determination of the electric field dependence of the effective critical current near voltage onset. In the vicinity of T_c, the critical current at low electric fields is observed to be actually enhanced over the limiting high-field value. The temperature dependence of J_c is found to be a relatively pure function of the reduced temperature $(1 - T/T_c)^n$, with n varying from about 1 for films prepared near the optimum oxygen-doping level, to more than 2 on either side of optimum.

ACKNOWLEDGMENTS

The author wishes to thank Dr. F. R. Fickett, Dr. A. T. Fiory, Professor A. Schmid, and Dr. A. F. Clark for useful discussions and correspondence.

---

*Support provided through the National Bureau of Standards Postdoctoral Research Associate Program in association with the National Research Council.

[1]See, for example, D. Dew-Hughes, in *Superconducting Machines and Devices, Large System Applications*, edited by S. Foner and B. B. Schwartz (Plenum, New York, (1974), Chap. 2, p. 109.

[2]A. A. Abrikosov, Zh. Eksp. Teor. Fiz. 32, 1442 (1957) [Sov. Phys.-JETP 5, 1174 (1957)].

[3]B. Abeles, R. W. Cohen, and G. W. Cullen, Phys. Rev. Lett. 17, 632 (1966); B. Abeles, R. W. Cohen, and R. W. Stowell, *ibid.* 18, 902 (1967); R. W. Cohen and B. Abeles, Phys. Rev. 168, 444 (1968).

[4]G. Deutscher, H. Fenichel, M. Gershenson, E. Grünbaum, and Z. Ovadyahu, J. Low Temp. Phys. 10, 231 (1973).

[5]The maximum deviation between values of T_c measured in these films and those reported by Deutscher *et al.* at the same ρ_n was less than 8%.

[6]See, for example, T. E. Faber and A. B. Pippard, Proc. R. Soc. A 231, 336 (1955); or F. R. Fickett, Cryogenics 11, 349 (1971).

[7]See, for example, Y. B. Kim and M. J. Stephen, in *Superconductivity*, edited by R. D. Parks (Marcel Dekker, New York, 1969), Chap. 19, p. 1128.

[8]Many thanks are extended to A. T. Fiory of Bell Laboratories for supplying this magnet.

[9]See Fig. 2 of A. Schmidt and W. Hauger, J. Low Temp. Phys. 11, 667 (1973).

[10]A. I. Larkin and Yu. N. Ovchinnikov, Zh. Eksp. Teor. Fiz. 65, 1704 (1973) [Sov. Phys.-JETP 38, 854 (1974)].

[11]The samples were immersed directly in a superfluid helium bath whose temperature was controlled to within 0.0001 K using a carbon thermometer and an ac-feedback-controlled heater. Absolute bath temperature was determined to within 1 mK with an oil manometer.

[12]See, for example, D. Saint-James, E. J. Thomas, and G. Sarma, *Type II Superconductivity* (Oxford U. P., Oxford, 1969).

[13]See, for example, Y. B. Kim and M. J. Stephen, in Ref. 7, p. 1120.